



HAL
open science

Climatic controls of decomposition drive the global biogeography of forest-tree symbioses

B. Steidinger, T. Crowther, J. Liang, M. van Nuland, G. Werner, B. Reich, G. Nabuurs, S. De-Miguel, M. Zhou, N. Picard, et al.

► **To cite this version:**

B. Steidinger, T. Crowther, J. Liang, M. van Nuland, G. Werner, et al.. Climatic controls of decomposition drive the global biogeography of forest-tree symbioses. *Nature*, 2019, 569 (7756), pp.404-408. 10.1038/s41586-019-1128-0 . hal-02147493

HAL Id: hal-02147493

<https://hal.science/hal-02147493v1>

Submitted on 4 Dec 2024

HAL is a multi-disciplinary open access archive for the deposit and dissemination of scientific research documents, whether they are published or not. The documents may come from teaching and research institutions in France or abroad, or from public or private research centers.

L'archive ouverte pluridisciplinaire **HAL**, est destinée au dépôt et à la diffusion de documents scientifiques de niveau recherche, publiés ou non, émanant des établissements d'enseignement et de recherche français ou étrangers, des laboratoires publics ou privés.



UNIVERSITY OF LEEDS

This is a repository copy of *Author Correction: Climatic controls of decomposition drive the global biogeography of forest-tree symbioses*.

White Rose Research Online URL for this paper:

<https://eprints.whiterose.ac.uk/167528/>

Version: Accepted Version

Article:

Steidinger, BS, Crowther, TW, Liang, J et al. (13 more authors) (2019) Author Correction: Climatic controls of decomposition drive the global biogeography of forest-tree symbioses. *Nature*, 571 (7765). E8. E8-. ISSN 0028-0836

<https://doi.org/10.1038/s41586-019-1342-9>

Copyright © 2019, The Author(s), under exclusive licence to Springer Nature Limited. This is an author produced version of a corrigendum published in *Nature*. Uploaded in accordance with the publisher's self-archiving policy.

Reuse

Items deposited in White Rose Research Online are protected by copyright, with all rights reserved unless indicated otherwise. They may be downloaded and/or printed for private study, or other acts as permitted by national copyright laws. The publisher or other rights holders may allow further reproduction and re-use of the full text version. This is indicated by the licence information on the White Rose Research Online record for the item.

Takedown

If you consider content in White Rose Research Online to be in breach of UK law, please notify us by emailing eprints@whiterose.ac.uk including the URL of the record and the reason for the withdrawal request.



eprints@whiterose.ac.uk
<https://eprints.whiterose.ac.uk/>

1 **Title:** Climatic controls of decomposition drive the global biogeography of forest tree
2 symbioses

3
4 **Authors:** Steidinger BS¹*, Crowther TW²†*, Liang J^{3,4}*, Van Nuland ME¹, Werner GDA⁵,
5 Reich PB^{6,7}, Nabuurs G⁸, de-Miguel S^{9,10}, Zhou M³, Picard N¹¹, Herault B¹², Zhao X⁴, Zhang C⁴,
6 Routh D², [Uploaded GFBi Author List], and Peay KG¹†

7
8 **Affiliations:**

9 ¹ Department of Biology, Stanford University, Stanford CA USA

10 ² Department of Environmental Systems Science, ETH Zürich, Zürich, Switzerland

11 ³ Department of Forestry and Natural Resources, Purdue University, West Lafayette, IN, USA

12 ⁴ Research Center of Forest Management Engineering of State Forestry Administration, Beijing
13 Forestry University, Beijing, China

14 ⁵ Department of Zoology, University of Oxford, Oxford UK

15 ⁶ Department of Forest Resources, University of Minnesota

16 ⁷ Hawkesbury Institute for the Environment, Western Sydney University

17 ⁸ Wageningen University and Research

18 ⁹ Departament de Producció Vegetal i Ciència Forestal, Universitat de Lleida-Agrotecnio Center

19 ¹⁰ Forest Science and Technology Centre of Catalonia (CTFC)

20 ¹¹ Food and Agriculture Organization of the United Nations

21 ¹² Cirad, INP-HB, Univ Montpellier, UPR Forêts et Sociétés

22
23 *These authors contributed equally to this work and share the first-author

24 †Corresponding authors: Email kpeay@stanford.edu; albeca.liang@gmail.com;
25 tom.crowther@usys.ethz.ch

26
27 **The identity of the dominant microbial symbionts in a forest determines the ability**
28 **of trees to access limiting nutrients from atmospheric or soil pools^{1,2}, sequester**
29 **carbon^{3,4} and withstand the impacts of climate change¹⁻⁷. Characterizing the global**
30 **distribution of symbioses, and identifying the factors that control it, are thus integral to**
31 **understanding present and future forest ecosystem functioning. Here we generate the first**
32 **spatially explicit map of forest symbiotic status using a global database of 1.2 million forest**
33 **inventory plots with over 28,000 tree species. Our analyses indicate that climatic variables,**
34 **and in particular climatically-controlled variation in decomposition rate, are the primary**
35 **drivers of the global distribution of major symbioses. We estimate that ectomycorrhizal**
36 **(EM) trees, which represent only 2% of all plant species⁸, constitute approximately 60% of**

37 tree stems on Earth. EM symbiosis dominates forests where seasonally cold and dry
38 climates inhibit decomposition, and are the predominant symbiosis at high latitudes and
39 elevation. In contrast, arbuscular mycorrhizal (AM) trees dominate aseasonally warm
40 tropical forests and occur with EM trees in temperate biomes where seasonally warm-and-
41 wet climates enhance decomposition. Continental transitions between AM and EM
42 dominated forests occur relatively abruptly along climate driven decomposition gradients,
43 which is likely caused by positive plant-microbe feedbacks. Symbiotic N-fixers, which are
44 insensitive to climatic controls on decomposition compared with mycorrhizal fungi, are
45 most abundant in arid biomes with alkaline soils and high maximum temperatures. The
46 climatically driven global symbiosis gradient we document represents the first spatially-
47 explicit, quantitative understanding of microbial symbioses at the global scale and
48 demonstrates the critical role of microbial mutualisms in shaping the distribution of plant
49 species.

50 Microbial symbionts strongly influence the functioning of forest ecosystems. They
51 exploit inorganic, organic² and/or atmospheric forms of nutrients that enable plant growth¹,
52 determine how trees respond to elevated CO₂⁶, regulate the respiratory activity of soil
53 microbes^{3,9}, and affect plant species diversity by altering the strength of conspecific negative
54 density dependence¹⁰. Despite growing recognition of the importance of root symbioses for
55 forest functioning^{1,6,11} and the potential to integrate symbiotic status into Earth system models
56 that predict functional changes to the terrestrial biosphere^{11,12}, we lack spatially-explicit,
57 quantitative maps of the different root symbioses at the global scale. Generating these
58 quantitative maps of tree symbiotic states would link the biogeography of functional traits of

59 belowground microbial symbionts with their 1.5 trillion host trees¹³, spread across Earth's
60 forests, woodlands, and savannas.

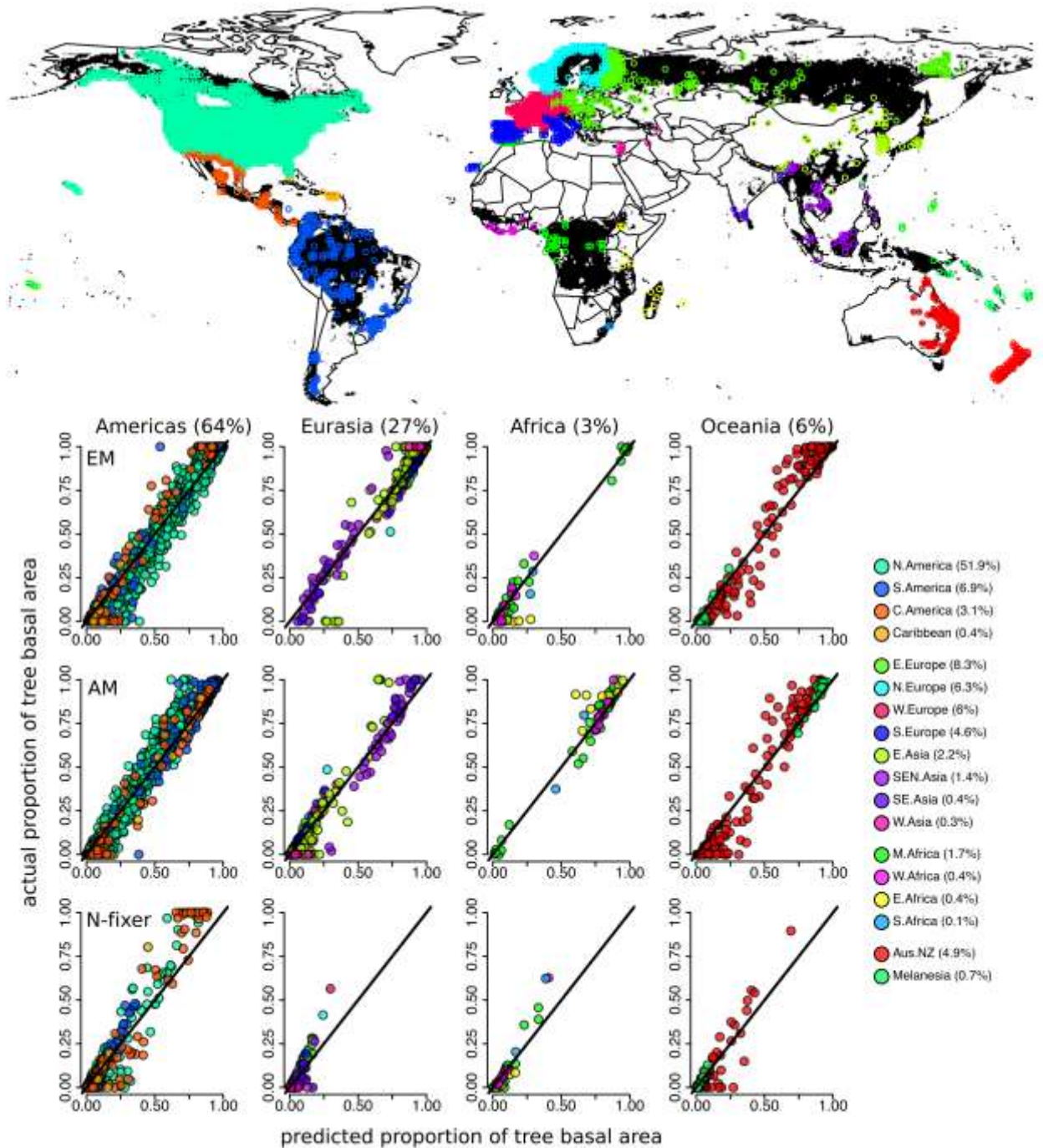
61 The dominant guilds of tree root symbionts, arbuscular mycorrhizal (AM) fungi,
62 ectomycorrhizal (EM) fungi, ericoid mycorrhizal (ErM) fungi, and nitrogen (N)-fixing bacteria
63 (N-fixer) are all based on the exchange of plant photosynthate for limiting macronutrients. The
64 AM symbiosis is the oldest of the four, having evolved nearly 500 million years ago, with EM,
65 ErM and N-fixer plant taxa having evolved multiple times from an AM basal state. Plants that
66 form the AM symbiosis are markedly more diverse than the other symbiotic groups, comprising
67 nearly 80% of all terrestrial plant species, and principally rely on AM fungi for enhancing
68 mineral phosphorus (P) uptake¹⁴. EM fungi evolved more recently from saprotrophic ancestors,
69 and as a result may be better than AM fungi at competing with free living soil microbes for
70 resources³. As such, some EM fungal lineages are more capable of mobilizing organic sources of
71 soil nutrients (particularly nitrogen) compared with AM fungi^{15,16}. Association with EM fungi,
72 but not AM fungi, has been shown to allow trees to accelerate photosynthesis in response to
73 increased atmospheric CO₂ when soil nitrogen (N) is limiting⁶ and to inhibit soil respiration by
74 decomposer microbes^{3,9} (but see ¹⁷). Because increased plant photosynthesis and decreased soil
75 respiration both reduce atmospheric CO₂ concentrations, the EM symbiosis is associated with
76 buffering the Earth's climate against anthropogenic changes.

77 In contrast to mycorrhizal fungi, which extract nutrients from the soil, symbiotic N-fixers
78 (Rhizobia and Actinobacteria) convert atmospheric N₂ to plant-usable forms. Symbiotic N-fixers
79 are responsible for a large fraction of biological soil-N inputs, which can increase N-availability
80 in forests where they are locally abundant¹⁸. Both N-fixing bacteria and EM fungi often demand
81 more plant photosynthate than does the AM symbiosis^{14,19,20}. Because tree growth and

82 reproduction are limited by access to inorganic, organic and atmospheric sources of N, the
83 distribution of these root symbioses is likely to reflect both environmental conditions that
84 maximize the cost-benefit ratio of symbiotic exchange as well as physiological constraints on
85 different symbionts.

86 In one of the earliest efforts to understand the functional biogeography of plant root
87 symbioses, Sir David Read²¹ categorically classified biomes by their perceived dominant
88 mycorrhizal type and hypothesized that seasonal climates favor hosts associating with EM fungi
89 due to their ability to compete directly for organic N. By contrast, it has been proposed that
90 sensitivity to low temperatures has prevented N-fixers from dominating outside the tropics,
91 despite the potential for N-fixation to alleviate N-limitation in boreal forests^{20,22}. However,
92 global scale tests of these proposed biogeographic patterns and their proposed climate drivers are
93 lacking or inconclusive²³⁻²⁵ and we have no understanding of the regional variations in this
94 proposed latitudinal trend. To address this research gap, we compiled the first global ground-
95 sourced survey database to reveal numerical abundances of each symbiosis across the global
96 forested biomes, rather than incidence (presence or absence, e.g.,²³⁻²⁵), which is essential for
97 identifying the shapes and potential mechanisms underlying transitions in forest symbiotic state
98 along climatic gradients^{26,27}.

99 We determined the abundance of tree symbioses using GFBi, an extension from the plot-
100 based Global Forest Biodiversity (GFB²⁸) database, which contains over 1.2 million forest
101 inventory plots of individual-based measurement records from which we derive abundance
102 information for entire tree communities (Figure 1).



103

104 **Figure 1.** A map of 1 by 1 degree grid cells where we analyzed the proportion of tree stems
 105 and basal area for different symbiotic guilds (above). Circles show the location of training
 106 data, colored by geographic origin, while black squares show the extent of model
 107 projections. Panels below the map show actual vs. predicted proportion of basal area for
 108 ectomycorrhizal (EM), arbuscular mycorrhizal (AM), and N-fixer trees by continent and
 109 subregion, and demonstrate globally consistent model performance.

110 Using published literature on the evolutionary histories of mycorrhizal and N-fixer
111 symbioses^{8,25,29-33}, we assigned plant species from the GFBi to one of 5 symbiotic guilds: AM,
112 EM, ErM, N-fixer, and non- or weakly-mycorrhizal (NM). Most plants with symbioses derived
113 from the AM state retain the genetic potential to associate with AM fungi¹⁴. Thus, consistent
114 with other studies in this field²⁹, we assigned tree species to the AM-exclusive guild if they were
115 not EM, ericoid mycorrhizal, non-mycorrhizal, or N-fixers. While there is some uncertainty in
116 such assignments, direct investigation of mycorrhizal status when done supports this
117 assumption³⁴. Because individual measurements of mycorrhizal colonization are not possible at
118 this scale, our models represent potential symbiotic associations.

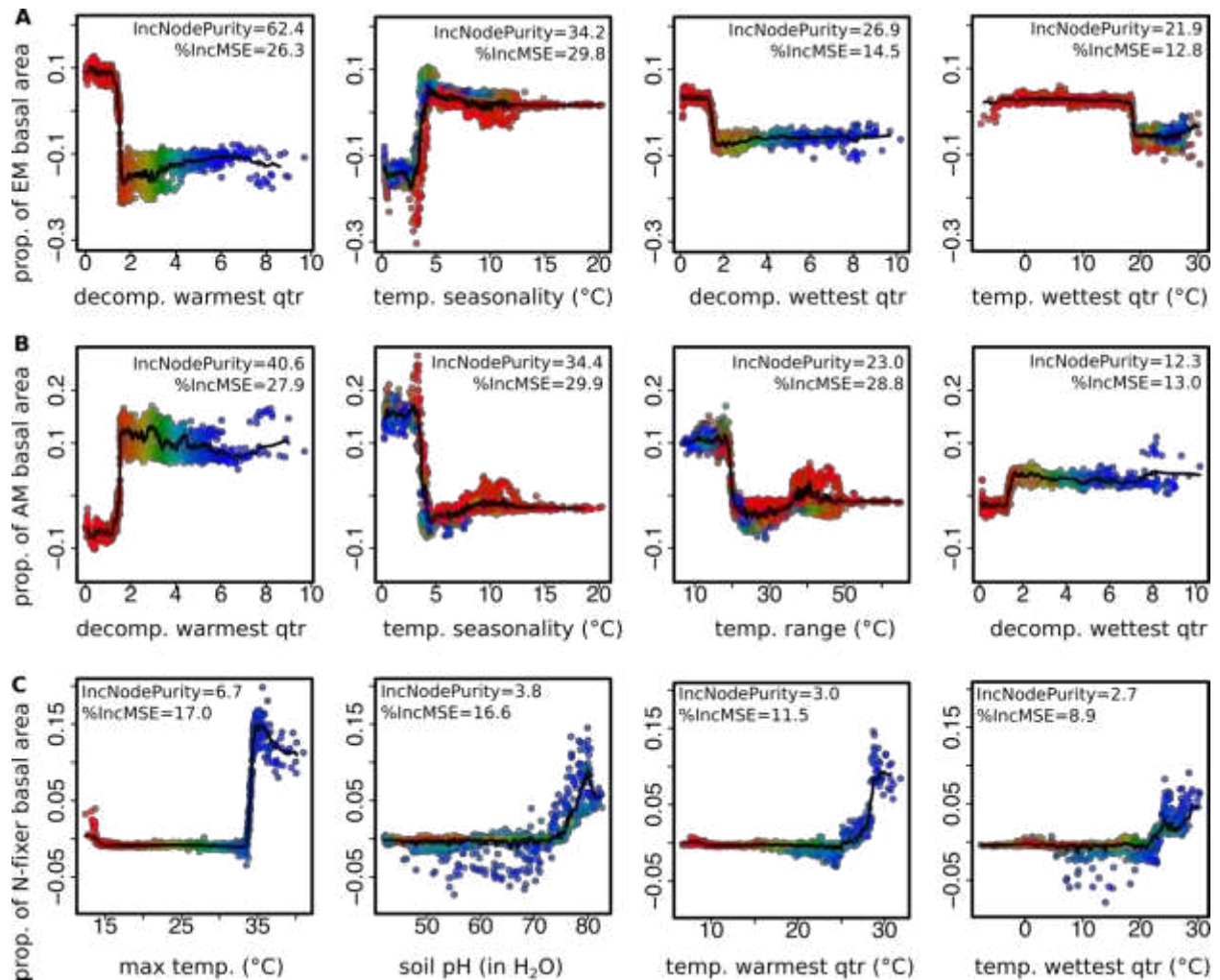
119 To identify the key factors structuring symbiotic distributions we assembled 70 global
120 predictor layers: 19 climatic (annual, monthly, and quarterly temperature and precipitation
121 variables), 14 soil chemical (total soil N density, microbial N, C:N ratios and soil P fractions,
122 pH, cation exchange capacity), 5 soil physical (soil texture and bulk density), 26 vegetative
123 indices (leaf area index, total stem density, enhanced vegetation index means and variances), and
124 5 topographic variables (elevation, hillshade) (Table S7). Because decomposition is the dominant
125 process by which soil nutrients become available to plants, we generated 5 additional layers that
126 estimate the climatic control of decomposition. We parameterized decomposition coefficients
127 according to the Yasso07 model^{35,36} using the following equation:

$$128 \quad k = \text{Exp}(0.095T_i - 0.00014 T_i^2) (1 - \text{Exp}[-1.21 P_i]), \quad (1)$$

129 where P_i and T_i are precipitation and mean temperature, either quarterly or annually, and the
130 constants $0.0095 (= \beta_1)$, $0.00014 (= \beta_2)$, and $-1.21 (= \gamma)$ are parameters fit using a previous global
131 study of leaf litter mass-loss³⁶. Although local decomposition rates can vary significantly based
132 on litter quality or microbial community composition³⁷, climate is the primary control at the

133 global scale³⁶. Decomposition coefficients describe how fast different chemical pools of leaf
134 litter lose mass over time relative to a parameter, α , that accounts for leaf-chemistry.
135 Decomposition coefficients (k) with values of 0.5 and 2 indicate a halving and doubling of
136 decomposition rates relative to α , respectively (Supplemental Materials).

137 Given the large set of possible environmental predictors, we used the random forest
138 machine-learning algorithm to identify the best predictors of global symbiosis distributions. The
139 random forest algorithm averages multiple regression trees, each of which uses a random subset
140 of all the model variables to predict a response. These regression trees identify optimal values
141 along a predictor-gradient to “split” the model response into different nodes (e.g., predictions
142 could be “split” into nodes of 50 or 75% of EM basal area depending on whether mean annual
143 temperature is $>$ or $<$ 20°C). We ranked the importance of each variable according to inc node
144 purity, which measures the decrease in model error that occurs whenever the response is split on
145 that variable (Figure 2ABC). We first determined the influence and relationship of all 75
146 predictor layers on forest symbiotic state and then optimized our models using a stepwise
147 reduction in variables, from least- to most-important. Soil chemical, vegetative, and topographic
148 variables were the first to be eliminated from our models in this way. In a subsequent model that
149 included only layers of climate, decomposition, and certain soil physical and chemical
150 information, we found that the 4 most important variables accounted for $>85\%$ of the explained
151 variability. We plot the partial-fits of these four variables for each symbiotic guild (Figure
152 2ABC).



153 **Figure 2.** Partial plots of residual variation explained by the four most important
 154 predictors of the proportion of tree basal area belonging to the (A) ectomycorrhizal (EM),
 155 (B) arbuscular mycorrhizal (AM), and (C) N-fixer symbiotic guilds. Variables are listed in
 156 declining importance from left to right, as determined by inc node purity, with points
 157 colored with a red-green-blue gradient according to their position on the x-axis of the most
 158 important variable (left-most panels for each guild), allowing cross visualization between
 159 predictors. Each panel lists two measures of variable importance, inc node purity (used for
 160 sorting) and %IncMSE (see Supplemental Information for description). Decomposition
 161 rates in (A) and (B) are in units of leaf litter mass loss per quarter. The abundance of each
 162 symbiont type transitions sharply along climatic gradients, suggesting that sites near the
 163 threshold are particularly vulnerable to switching their dominant symbiont guild with
 164 climate changes.

165

166 The three most numerically abundant tree symbiotic guilds each have reliable
 167 environmental signatures, with the four most important predictors accounting for 81, 79, and
 168 52% of the total variability in EM, AM, and N-fixer relative basal area, respectively. Models for

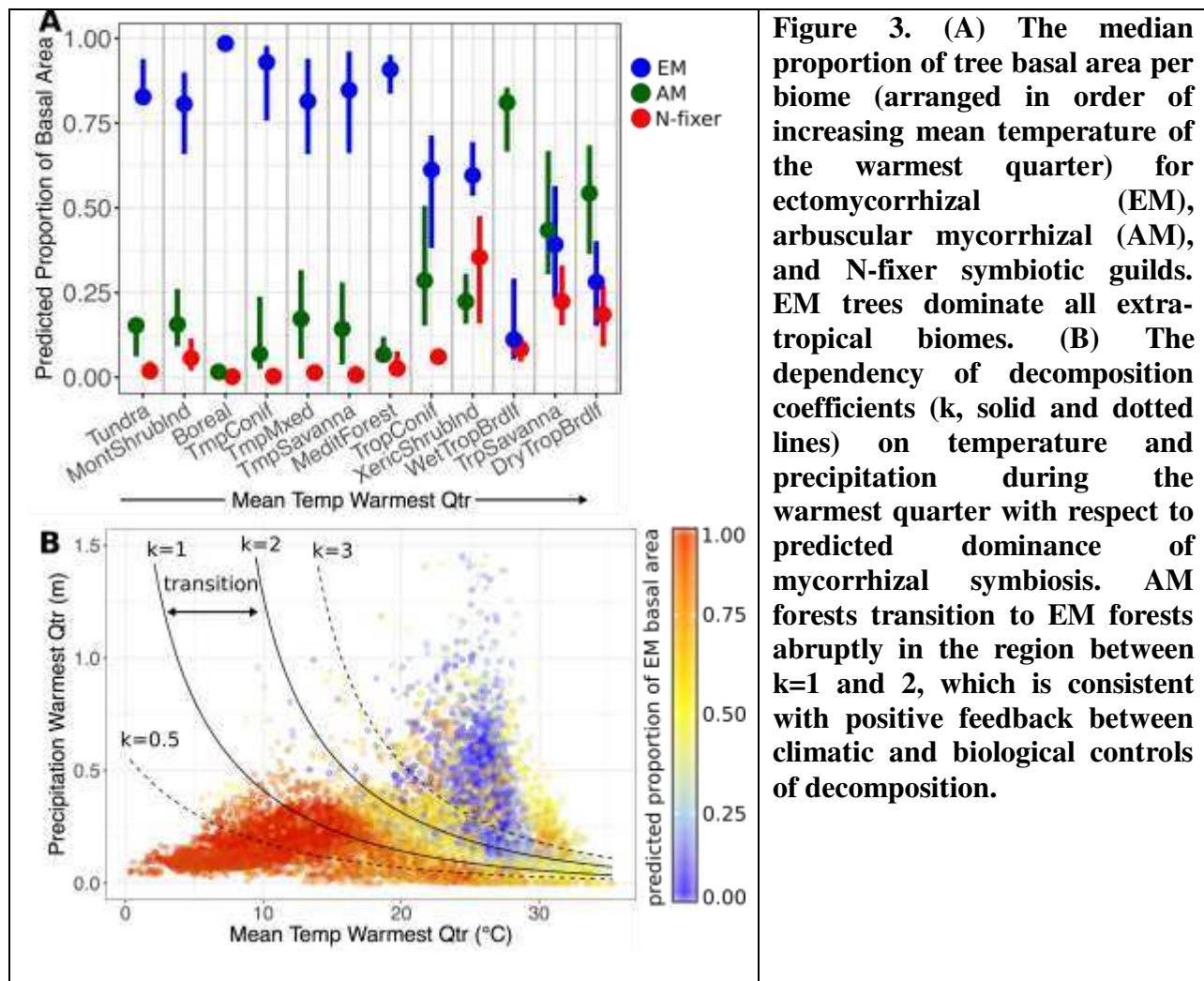
169 ErM and NM lack strong predictive power given the relative rarity of these symbiotic states
170 amongst trees, although the raw data do identify some local abundance hotspots for ErM (Figure
171 S1). As a result, we focus the remainder of results and discussion on the three major tree
172 symbiotic states (EM, AM, N-fixer). Despite the fact that data from N. and S. America constitute
173 65% of the training data (at the 1 by 1 degree grid scale), our models accurately predict the
174 proportional abundances of the three major symbioses across all major geographic regions
175 (Figure 1). The high performance of our models, which is robust to both K-fold cross-validation
176 and rarefying samples so that all continents are represented with equal depth (Figures S10-12),
177 suggest that regional variations in climate (including indirect effects on decomposition) and soil
178 pH (for N-fixers) are the primary factors influencing the relative dominance of each guild at the
179 global scale (geographic origin only explained ~2-5% of the variability in residual relative
180 abundance) (Figure 1BCD, Table S8).

181 Random forest models should not be projected across predictor gradients that fall outside
182 the ranges of their training data (e.g., grid cells with higher mean annual temperatures than the
183 maximum used to fit the models). To prevent the over-projecting of our models over pixels
184 where we lacked training data, we subset a global grid of predictor layers depending on whether
185 (1) the grid cell fell within the top 60% of land surface with respect to tree stem density¹³ and
186 either (2) fell within the univariate distribution of all the predictor layers from our training data
187 and/or (3) fell within an 8-dimensional hypervolume defined by the unique set of the 4-best
188 predictors of the relative abundance of each guild (Figure 2, Supplemental Materials). We then
189 projected our models across only those grid cells that met these criteria, which constitutes 46%
190 of the global land surface and 88% of global tree stems (Figure 1; Figure S16). While model
191 validation indicates that our projections are robust, additional ground truthing of predictions to

192 identify any discrepancies would be incredibly valuable. If such discrepancies exist they can
193 help fine tune climate-symbiosis models, or identify areas where climate might favor invasion
194 by symbioses that have not yet evolved or dispersed to a particular biogeographic region.

195 In contrast to a recent global analysis of root traits, which concluded that plant evolution
196 has favored reduced dependence on mycorrhizal fungi³⁸, we find that trees associating with the
197 relatively more C-demanding and recently-derived EM fungi^{14,19} represent the dominant tree-
198 symbiosis. By taking the average proportion of EM trees, weighted by spatially-explicit global
199 predictions for tree stem density¹³, we estimate that approximately 60% of trees on earth are EM,
200 despite the fact that only 2% of plant species associate with EM fungi (vs. 80% associating with
201 AM fungi)^{8,29}. Outside of the tropics, the estimate for EM relative abundance increases to
202 approximately 80% of trees.

203 Turnover among the major symbiotic guilds results in a tri-modal latitudinal abundance
204 gradient, with the proportion of EM trees increasing (and AM trees decreasing) with distance
205 from the equator, while N-fixing trees reach peak abundance in the arid zone around 30 degrees
206 (Figure 3A, Figure 4). These trends are driven by abrupt transitional regions along continental
207 climatic gradients (Figure 2), which skew the distribution of symbioses among biomes (Figure
208 3A) and drive strong patterns across geographic and topographic features that influence climate.
209 For example, moving north or south from the equator, the first transitional zone separates warm
210 (aseasonal), AM-dominated, tropical broadleaf forests (>75% median basal area, vs. 8% for EM
211 trees) from the rest of the EM-dominated world forest system (Figure 2AB; Figure 3A). It
212 stretches longitudinally across 25 degrees N and S, just beyond the dry tropical broadleaf forests
213 (with 25% EM tree basal area; Figure 3A), where average monthly temperature variation reaches
214 3-5°C (Figure 2AB).



215 Moving further N or S, the second transitional climate zone separates regions where
 216 decomposition coefficients during the warmest quarter of the year are less than 2 (see Figure 3B
 217 for the associated temperature and precipitation ranges). In N. America and China, this transition
 218 zone spans longitudinally around 50 degrees N, separating the mixed AM / EM temperate forests
 219 from their neighboring EM dominated boreal forests (75 vs 100% EM tree basal area,
 220 respectively; Figure 3A). This transitional decomposition zone bypasses W. Europe, which has
 221 temperature seasonality $> 5^{\circ}\text{C}$, but lacks sufficiently wet summers to accelerate decomposition
 222 coefficients beyond values associated with mixed AM/EM forests. The latitudinal transitions in
 223 symbiotic state observed among biomes are mirrored by within-biome transitions along elevation

224 gradients. For example, in tropical Mexico, warm and wet quarter decomposition coefficients <
225 2 occur along the slopes of the Sierra Madre, where mixed AM-exclusive and N-fixer woodlands
226 in arid climates transition to EM dominated tropical coniferous forests (75% basal area, Figure
227 3A, Figure 4ABC, Figure S17-19). The southern hemisphere, which lacks the landmass to
228 support extensive boreal forests, experiences a similar latitudinal transition in decomposition
229 rates along the ecotone separating its tropical and temperate biomes, around 28 degrees S.

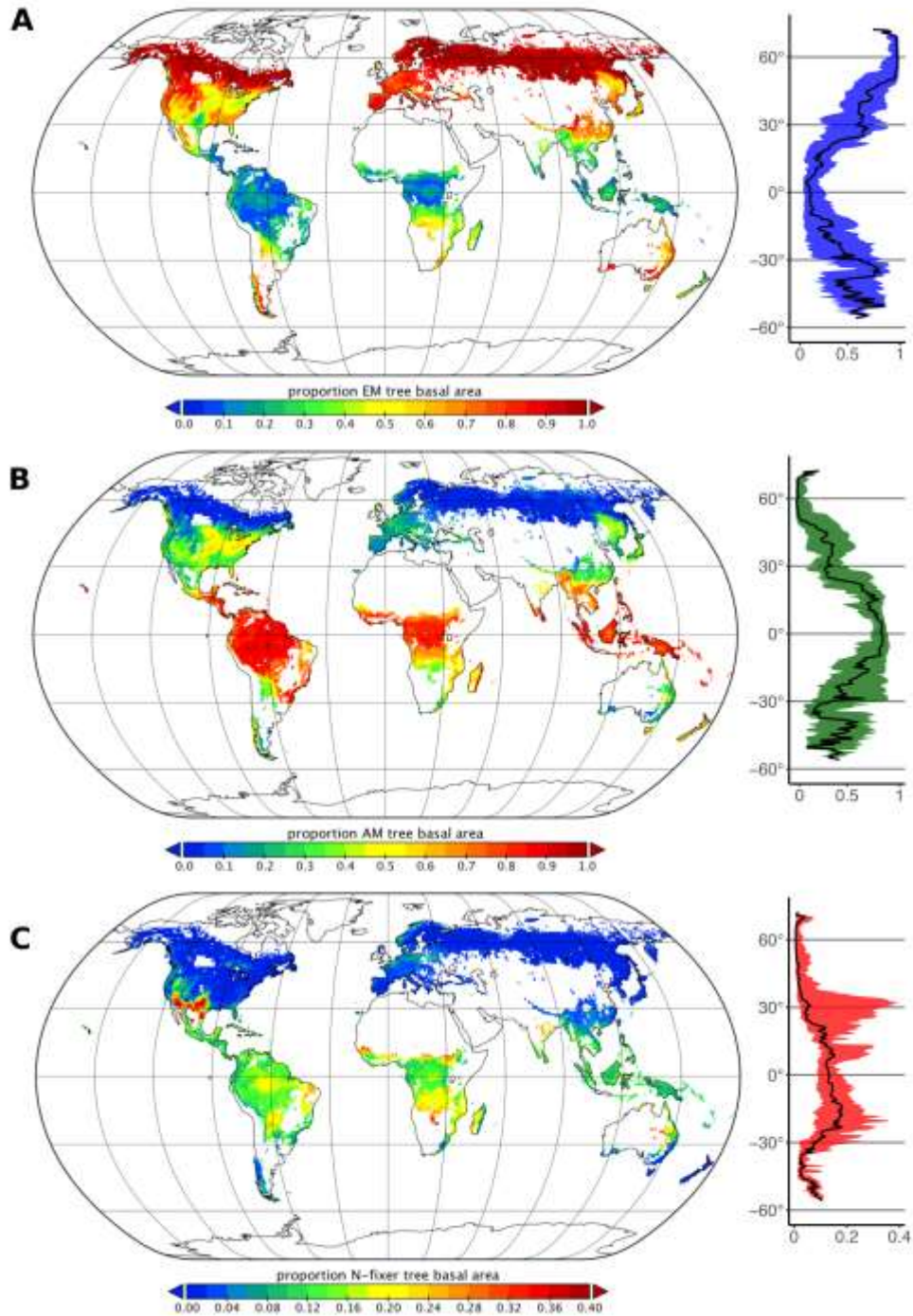
230 The abrupt transitions that we detected between forest symbiotic states along
231 environmental gradients suggest that positive feedbacks may exist between climatic and
232 biological controls of decomposition^{11,36}. In contrast to AM fungi, some EM fungi can use
233 oxidative enzymes to mineralize organic nutrients from leaf litter, converting nutrients to plant-
234 usable forms before transferring them to their host trees^{2,5}. Relative to AM trees, the leaf litter of
235 EM trees is also chemically more resistant to decomposition, with higher C:N ratios and higher
236 concentrations of decomposition-inhibiting secondary compounds¹¹. Thus, EM leaf litter can
237 exacerbate climatic barriers to decomposition, promoting conditions where EM fungi have
238 superior nutrient-acquiring abilities to AM-fungi^{5,11}. Such positive-feedbacks are known to cause
239 abrupt ecosystem transitions along smooth environmental gradients between woodlands and
240 grasses: trees suppress fires, which promotes seedling recruitment, while grass fuels fires, which
241 kill tree seedlings³⁹. Our study provides the first evidence that rapid transitions in tree
242 community structure along climate gradients could also be governed by positive-feedbacks
243 between symbiotic guilds and nutrient cycling; although other types of interactions, such as
244 environmentally sensitive competition hierarchies among symbiotic guilds, could also lead to
245 abrupt transitions without specifically invoking feedback effects. In either case, the existence of
246 abrupt transitions suggests that trees and associated microbial symbionts in transitional regions

247 along decomposition gradients should be susceptible to drastic turnover in symbiotic state with
248 future environmental changes⁴⁰.

249 To illustrate the sensitivity of global patterns of tree symbiosis to climate change, we use
250 the climate relationships we developed for current climate to project potential changes due to
251 climate change. Relative to our global predictions using the most recent climate data, model
252 predictions using the projected climates for 2070 suggest the abundance of EM trees will decline
253 by as much as 10% (using a relative concentration pathway of 8.5 W/m²; Figure S25). Due to
254 their position along decomposition gradients relative to the abrupt shift from EM to AM forests
255 (Figure 2AB), our models predict the largest declines in EM abundance will occur along the
256 boreal-temperate ecotone, although declines in species abundances can lag decades, or even
257 centuries or millennia, behind associated climatic changes⁴¹. The predicted decline in EM trees
258 corroborates the results of common garden transfer and simulated warming experiments, which
259 demonstrate that some important EM hosts will decline at the boreal-temperate ecotone in altered
260 climates⁴²⁻⁴⁴. Because of the low tree diversity in boreal forests, tree species loss around
261 transition zones may have major consequences for forest related economic activity⁴⁵.

262

263



264

265 **Figure 4. Predicted global maps (left) and latitudinal gradients (right, with solid line**
 266 **indicating the median and colored ribbon spanning the range from the 5% and 95%**
 267 **quantiles) of the proportion of tree basal area for (A) ectomycorrhizal (EM), (B)**
 268 **arbuscular mycorrhizal (AM), and (C) N-fixer symbiotic guilds.**
 269

270 The change in dominant nutrient exchange symbioses along climate gradients highlights
271 the interconnection between atmospheric and soil compartments of the biosphere. The transition
272 from AM to EM dominance corresponds with a shift from P to N limitation of plant growth with
273 increasing latitude⁴⁶⁻⁴⁸. Including published global projections of total soil N or P, microbial N,
274 or soil P fractions (labile, occluded, organic, and apatite) did not increase the amount of variation
275 explained by the model or alter the variables identified as most important, and thus were dropped
276 from our analysis. However, this does not necessarily mean that soil nutrient availability is
277 unimportant at the global scale, as the best-available global data likely do not adequately
278 represent local nutrient availability^{49,50}. Rather, our finding that climatic controls of
279 decomposition best predict the dominant mycorrhizal associations mechanistically links
280 symbiont physiology with climatic controls of soil nutrient release from leaf litter. These
281 findings are consistent with Read's hypothesis²¹ that slow decomposition at high latitudes favors
282 EM fungi due to their increased capacity to liberate organic nutrients². Thus, while more
283 experiments are necessary to understand the specific mechanism by which nutrient competition
284 favors dominance of AM or EM symbioses²⁶, we propose that the latitudinal and elevational
285 transitions from AM to EM dominated forests be called Read's Rule.

286 While our analyses focus on prediction at large spatial scales appropriate to the available
287 data, our findings with respect to Read's Rule also provide insight into how soil factors structure
288 the fine-scale distributions of tree symbioses within our grid cells. For example, while at a coarse
289 scale we find that EM trees are relatively rare in many wet tropical forests, individual tropical
290 sites in our raw data span the full range from 0 – 100 % EM basal area. In much of the wet
291 tropics, these EM dominated sites exist as outliers within a matrix of predominantly AM trees. In
292 an apparent exception that proves Read's Rule, in aseasonal warm neotropical climates, which

293 accelerate leaf-decomposition and promote regional AM dominance (Figure 3), EM dominated
294 tree stands can develop in sites where poor soils and recalcitrant litter slow decomposition and N
295 mineralization^{26,51}. Landscape-scale variation in the relative abundance of symbiotic states also
296 changes along climate gradients, with variability highest in xeric and temperate biomes (Figure
297 S2), suggesting that the potential of local nutrient variability to favor particular symbioses is
298 contingent on climate.

299 Whereas EM trees are associated with ecosystems where plant growth is thought to be
300 primarily N-limited, N-fixer trees are not. Our results highlight the global extent of the “N-
301 cycling paradox,” wherein some metrics suggest that N-limitation is greater in the temperate
302 zone⁴⁶⁻⁴⁸, yet N-fixing trees are relatively more common in the tropics^{20,52,53} (Figure 3A). We
303 find that N-fixers, which we estimate represent 7% of all trees, dominate forests with annual max
304 temperatures >35°C and alkaline soils (particularly in North America and Africa, Figure 2C).
305 They have the highest relative abundance in xeric shrublands (24%), tropical savannas (21%),
306 and dry broadleaf forest biomes (20%), but are nearly absent from boreal forests (<1%) (Figure
307 3A, Figure 4). The decline in N-fixer tree abundance we observed with increasing latitude is also
308 associated with a previously documented latitudinal shift in the identity of N-fixing microbes,
309 from facultative N-fixing rhizobial bacteria in tropical forests to obligate N-fixing actinorhizal
310 bacteria in temperate forests⁵². Our data are not capable of fully disentangling the several
311 hypotheses that have been proposed to reconcile the N-cycling paradox^{20,54}. However, our results
312 are consistent with the model prediction²² and regional empirical evidence^{27,55,56} that N-fixing
313 trees are particularly important in arid biomes. Based primarily on the observed positive,
314 nonlinear association of N-fixer relative abundance with the mean temperature of the hottest

315 month (Figure 2C), our models predict a two-fold increase in N-fixer relative abundance when
316 transitioning from humid to dry tropical forest biomes (Figure 3A).

317 Although soil microbes are a dominant component of forests, both in terms of diversity
318 and ecosystem functioning^{5,6,11}, identifying global-scale microbial biogeographic patterns
319 remains an ongoing research priority. Our analyses confirm that Read's Rule, which is one of the
320 first proposed biogeographic rules specific to microbial symbioses, successfully describes global
321 transitions between mycorrhizal guilds. More generally, climate driven turnover among the
322 major plant-microbe symbioses represents a fundamental biological pattern in the Earth system,
323 as forests transition from low-latitude arbuscular mycorrhizal, to N-fixer, to high-latitude
324 ectomycorrhizal ecosystems. The predictions of our model (which we make available as a global
325 raster layer) can now be used to represent these critical ecosystem variations in global
326 biogeochemical models used to predict climate-biogeochemical feedbacks within and between
327 trees, soils, and the atmosphere. Additionally, the layer containing the proportion abundance of
328 N-fixing trees can be used to map potential symbiotic N-fixation, which links together
329 atmospheric pools of C and N. Future work can extend our findings to incorporate multiple plant
330 growth forms and non-forested biomes, where similar patterns likely exist, to generate a
331 complete global perspective. Our predictive maps leverage the most comprehensive global forest
332 dataset to generate the first quantitative global map of forest tree symbioses, demonstrating how
333 nutritional mutualisms are coupled with the global distribution of plant communities.

334 **Acknowledgments**

335 This work is supported in part by the Key Project of National Key Research and Development
336 Plan, China (2017YFC0504005); the new faculty start-up grant, Department of Forestry and
337 Natural Resources, Purdue University; Dept. of Energy (DOE) Biological and Environmental

338 Research Program Early Career Research Grant DE-SC0016097; DOB Ecology, Plant-for-the-
339 Planet and the German Ministry for Economic Development and Cooperation; São Paulo
340 Research Foundation, #2014/14503-7; São Paulo Research Foundation (FAPESP), #2003/12595-
341 7; Proyecto FONACIT No. 1998003436 and UNELLEZ No. 23198105; EU, Sumforest –
342 REFORM, Risk Resilient Forest Management, FKZ: 2816ERA02S; U.S. National Science
343 Foundation Long-Term Ecological Research grant DEB-1234162, German Science Foundation
344 (DFG), KROOF Tree and stand-level growth reactions on drought in mixed versus pure forests
345 of Norway spruce and European beech, PR 292/12-1; Bavarian State Ministry for Food,
346 Agriculture and Forestry, W07 longterm yield experiments, 7831-26625-2017 and Project No
347 E33; The Deutsche Forschungsgemeinschaft (DFG) Priority Program 1374 Biodiversity
348 Exploratories; The International Tropical Timber Organization, ITTO-Project PD 53/00 Rev.3
349 (F); The State Forest Management Centre, Estonia, and the Environmental Investment Centre,
350 Estonia; Natural Sciences and Engineering Research Council of Canada Discover Grant Project
351 (RGPIN-2014-04181 and STPGP428641); European Structural Funds by FEDER 2014-2020
352 GY0006894; European Investment Funds by FEDER/COMPETE/POCI-Operational
353 Competitiveness and Internationalization Programme, under Project POCI-01-0145-FEDER-
354 006958 and National Funds by FCT - Portuguese Foundation for Science and Technology, under
355 the project UID/AGR/04033/2013; Vietnam National Foundation for Science and Technology
356 Development (NAFOSTED-106-NN.06-2016.10); German Research Foundation (DFG, FOR
357 1246); The project LIFE+ ForBioSensing PL Comprehensive monitoring of stand dynamics in
358 Bialowieza Forest co-funded by Life Plus (contract number LIFE13 ENV/PL/000048) and the
359 National Fund for Environmental Protection and Water Management in Poland (contract number
360 485/2014/WN10/OP-NM-LF/D); National Natural Scientific Foundation of China (31660055

361 and 31660074); The Polish State Forests National Forest Holding (2016); The Dutch Ministry of
362 Economic Affairs for funding the Dutch National Forest Inventory; The Grant 11-TE11-0100
363 from the U.S. National Space and Aeronautics Administration; the Tropical Ecology,
364 Assessment, and Monitoring (TEAM) / Conservation International project for funding the data
365 collection, and the National Institut Research Amazon (INPA); The Ministère des Forêts, de la
366 Faune et des Parcs du Québec (Canada); The Exploratory plots of FunDivEUROPE received
367 funding from the European Union Seventh Framework Programme (FP7/2007-2013) under grant
368 agreement 265171; DBT, Govt. of India through the project 'Mapping and quantitative
369 assessment of geographic distribution and population status of plant resources of Eastern
370 Himalayan region' (sanction order No. BT/PR7928/NDB/52/9/2006 dated 29th September 2006);
371 The financial support from Natural Sciences and Engineering Research Council of Canada to S.
372 Dayanandan; Czech Science Foundation Standard Grant (16-09427S) and European Research
373 Council advanced grant (669609); RFBR #16-05-00496; The project implementation
374 Demonstration object on the transformation of declining spruce forests into ecologically more
375 stable multifunctional ecosystems, ITMS 26220220026, supported by the Research &
376 Development Operational Program funded by the ERDF; The Swedish NFI, Department of
377 Forest Resource Management, Swedish University of Agricultural Sciences SLU; The National
378 Research Foundation (NRF) of South Africa (89967 and 109244) and the South African
379 Research Chair Initiative; University Research Committee of the University of the South Pacific,
380 and New Colombo Plan Funding through the Department of Foreign Affairs and Trade of the
381 Australian government; The TEAM project in Uganda supported by the Moore foundation and
382 Buffett Foundation through Conservation International (CI) and Wildlife Conservation Society
383 (WCS); COBIMFO project funded by the Belgian Science Policy Office (Belspo), contract no.

384 SD/AR/01A; The German Federal Ministry of Education and Research (BMBF) under Grant
385 FKZ 01LL0908AD for the project “Land Use and Climate Change Interactions in the Vu Gia
386 Thu Bon River Basin, Central Vietnam” (LUCCI); Programme Tropenbos Côte d'Ivoire : projet
387 04/97-1111a du “Complément d’Inventaire de la Flore dans le Parc National de Tai”; The Danish
388 Council for Independent Research | Natural Sciences (TREECHANGE, grant 6108-00078B to
389 JCS) and VILLUM FONDEN (grant 16549); ERC Advanced Grant 291585 (“T-FORCES”) and
390 a Royal Society-Wolfson Research Merit Award; RAINFOR plots supported by the Gordon and
391 Betty Moore Foundation and the U.K. Natural Environment Research Council (NERC), notably
392 NERC Consortium Grants ‘AMAZONICA’ (NE/F005806/1), ‘TROBIT’ (NE/D005590/1), and
393 ‘BIO-RED’ (NE/N012542/1); Fundação de Amparo à Pesquisa e Inovação de Santa Catarina,
394 FAPESC (2016TR2524), Conselho Nacional de Desenvolvimento Científico e Tecnológico,
395 CNPq [312075/2013-8]; “Investissement d’Avenir” grant managed by Agence Nationale de la
396 Recherche (CEBA, ref. ANR- 10-LABX-25-01); CIFOR's Global Comparative Study on
397 REDD+ funded by the Norwegian Agency for Development Cooperation (Norad), the Australian
398 Department of Foreign Affairs and Trade (DFAT), the European Union (EU), the International
399 Climate Initiative (IKI) of the German Federal Ministry for the Environment, Nature
400 Conservation, Building and Nuclear Safety (BMUB), and the CGIAR Research Program on
401 Forests, Trees and Agroforestry (CRP-FTA), and donors to the CGIAR Fund; The Nature and
402 Biodiversity Conservation Union (NABU) under the project entitled “Biodiversity under Climate
403 Change: Community Based Conservation, Management and Development Concepts for the Wild
404 Coffee Forests”, funded by the German Federal Ministry for the Environment, Nature
405 Conservation and Nuclear Safety (BMU) through the International Climate Initiative (IKI); The
406 Conselho Nacional de Desenvolvimento Científico e Tecnológico (CNPq); The institutional

407 project “EXTEMIT - K”, no. CZ.02.1.01/0.0/0.0/15_003/0000433 financed by OP RDE; EC DG
408 VIII grant BZ-5041 (ECOSYN), NWO-WOTRO (W84-204), and GTZ; AfriTRON network
409 plots funded by the local communities and NERC, ERC, European Union, Royal Society and
410 Leverhume Trust; BOLFOR (Proyecto de Manejo Forestal Sostenible- Bolivia); The Global
411 Environment Research Fund F-071 and D-1006, and JSPS KAKENHI Grant Numbers
412 JP17K15289; The National Institute of Biology(Now Research Center for Biology), LIPI
413 (Indonesian Institute of Sciences), Indonesia IFBN project (contract 4000114425/15/NL/FF/gp)
414 funded by ESA; NSF grant DBI-1565046; Swiss National Science Foundation (SNSF No.
415 130720, 147092); Projects D/9170/07, D/018222/08, D/023225/09 and D/032548/10 funded by
416 the Spanish Agency for International Development Cooperation [Agencia Española de
417 Cooperación Internacional para el Desarrollo (AECID)] and Fundación Biodiversidad, in
418 cooperation with the Universidad Mayor de San Simón (UMSS), the FOMABO (Manejo
419 Forestal en las Tierras Tropicales de Bolivia) project and CIMAL (Compañía Industrial
420 Maderera Ltda.); The Agency for Economic and Environmental Development (DDEE) of the
421 north province of New Caledonia (the projects Ecofor & Cogefor, 2011-2016); Russian Science
422 Foundation (16-17-10284 “The accumulation of carbon in forest soils and forest succession
423 status”); Norwegian Ministry of Food and Agriculture; A grant from the Royal Society and the
424 Natural Environment Research Council (UK) to S.L.L.; The Spanish Agency for International
425 Development Cooperation [Agencia Española de Cooperación Internacional para el Desarrollo
426 (AECID)] and Fundación Biodiversidad, in cooperation with the governments of Syria and
427 Lebanon; COBIMFO Project, Federal Science Policy, Belgium; Consejo Nacional de Ciencia y
428 Tecnología, Mexico; Comisión Nacional Forestla, Mexico; BEF-China project (FOR 891)
429 funded by the German Research Foundation (DFG); WWF Russell Train Fellowship to P.M.U.

430 (Grant ST54); Wildlife Conservation Society DRC Program under CARPE Funding; Seoul
431 National University Big Data Institute through the Data Science Research Project 2016, R&D
432 Program for Forest Science Technology (Project No. 2013069C10-1719-AA03 &
433 S111215L020110) funded by Korea Forest Service (Korea Forestry Promotion Institute); The
434 European Union's Horizon 2020 research and innovation program within the framework of the
435 MultiFUNGtionality Marie Skłodowska-Curie Individual Fellowship (IF-EF) under grant
436 agreement 655815; Tropenbos International-Suriname; The Institute for World Forestry,
437 University of Hamburg; REMBIOFOR Project "Remote sensing based assessment of woody
438 biomass and carbon storage in forests" funded by The National Centre for Research and
439 Development, Warsaw, Poland, under the BIOSTRATEG program (agreement no.
440 BIOSTRATEG1/267755/4/NCBR/2015); The National Science Centre, Poland (Grant:
441 2011/02/A/NZ9/00108); Project "Environmental and genetic factors affecting productivity of
442 forest ecosystems on forest and post-industrial habitats" (2011-2015; no. OR/2717/3/11); Project
443 "Carbon balance of the major forest-forming tree species in Poland" (2007-2011; no. 1/07)
444 funded by the General Directorate of State Forests, Warsaw, Poland; and the research
445 professorship for "Ecosystem-based sustainable development" funded by Eberswalde University
446 for Sustainable Development. GK was supported by an Alexander von Humboldt fellowship.
447 GDAW was supported from a Newton International Fellowship from the Royal Society.

448

449 We thank the following agencies, initiatives, teams, and individuals for data collection and other
450 technical support: the Global Forest Biodiversity Initiative (GFBI) for establishing the data
451 standards and collaborative framework; United States Department of Agriculture, Forest Service,
452 Forest Inventory and Analysis (FIA) Program; University of Alaska Fairbanks; The SODEFOR,

453 Ivory Coast; the Queensland Herbarium and past Queensland Government Forestry and Natural
454 Resource Management Departments and staff for data collection for over seven decades. Ziaur
455 Rahman Laskar, Salam Dilip, Bijit, Bironjoy and Samar; Badru Mugerwa and Emmanuel
456 Akampurira, together with a team of field assistants (Valentine and Lawrence); all persons who
457 made the Third Spanish Forest Inventory possible, especially the main coordinator, J. A.
458 Villanueva (IFN3); Italian and Friuli Venezia Giulia Forest Services (Italy); Rafael Ávila and
459 Sharon van Tuylen, Insituto Nacional de Bosques (INAB), Guatemala for facilitating
460 Guatemalan data; The National Focal Center for Forest condition monitoring of Serbia (NFC),
461 Institute of Forestry, Belgrade, Serbia; The Thünen Institute of Forest Ecosystems (Germany) for
462 providing National Forest Inventory data; All TEAM data provided by the Tropical Ecology
463 Assessment and Monitoring (TEAM) Network, a collaboration between Conservation
464 International, the Missouri Botanical Garden, the Smithsonian Institution, and the Wildlife
465 Conservation Society, and partially funded by these institutions, the Gordon and Betty Moore
466 Foundation, and other donors, with thanks to all current and previous TEAM site manager and
467 other collaborators that helped collecting data; The people of the Redi Doti, Pierrekondre and
468 Cassipora village who were instrumental in assisting with the collection of data and sharing local
469 knowledge of their forest; and the dedicated members of the field crew of Kabo 2012 census.
470 Yadvinder Malhi's contribution was supported by an ERC Advanced Investigator Award GEM-
471 TRAILS (321131).

472 **References**

- 473 1 Batterman, S. A. *et al.* Key role of symbiotic dinitrogen fixation in tropical forest
474 secondary succession. *Nature* **502**, 224-227, doi:10.1038/nature12525 (2013).
475 2 Shah, F. *et al.* Ectomycorrhizal fungi decompose soil organic matter using oxidative
476 mechanisms adapted from saprotrophic ancestors. *New Phytol* **209**, 1705-1719,
477 doi:10.1111/nph.13722 (2016).

- 478 3 Averill, C., Turner, B. L. & Finzi, A. C. Mycorrhiza-mediated competition between
479 plants and decomposers drives soil carbon storage. *Nature* **505**, 543-+,
480 doi:10.1038/nature12901 (2014).
- 481 4 Clemmensen, K. E. *et al.* Roots and associated fungi drive long-term carbon
482 sequestration in boreal forest. *Science* **339**, 1615-1618, doi:10.1126/science.1231923
483 (2013).
- 484 5 Cheeke, T. E. *et al.* Dominant mycorrhizal association of trees alters carbon and nutrient
485 cycling by selecting for microbial groups with distinct enzyme function. *New Phytol.*
486 **214**, 432-442, doi:10.1111/nph.14343 (2017).
- 487 6 Terrer, C., Vicca, S., Hungate, B. A., Phillips, R. P. & Prentice, I. C. Mycorrhizal
488 association as a primary control of the CO₂ fertilization effect. *Science* **353**, 72-74,
489 doi:10.1126/science.aaf4610 (2016).
- 490 7 Johnson, D. J., Beaulieu, W. T., Bever, J. D. & Clay, K. Conspecific negative density
491 dependence and forest diversity. *Science* **336**, 904-907 (2012).
- 492 8 Brundrett, M. C. in *Biogeography of Mycorrhizal Symbiosis* 533-556 (Springer, 2017).
- 493 9 Averill, C. & Hawkes, C. V. Ectomycorrhizal fungi slow soil carbon cycling. *Ecol Lett*
494 **19**, 937-947, doi:10.1111/ele.12631 (2016).
- 495 10 Bennett, J. A. *et al.* Plant-soil feedbacks and mycorrhizal type influence temperate forest
496 population dynamics. *Science* **355**, 181-184 (2017).
- 497 11 Phillips, R. P., Brzostek, E. & Midgley, M. G. The mycorrhizal-associated nutrient
498 economy: a new framework for predicting carbon-nutrient couplings in temperate forests.
499 *New Phytol.* **199**, 41-51, doi:10.1111/nph.12221 (2013).
- 500 12 Oleson, K. W. *et al.* Technical description of version 4.0 of the Community Land Model
501 (CLM). (2010).
- 502 13 Crowther, T. W. *et al.* Mapping tree density at a global scale. *Nature* **525**, 201 (2015).
- 503 14 Heijden, M. G., Martin, F. M., Selosse, M. A. & Sanders, I. R. Mycorrhizal ecology and
504 evolution: the past, the present, and the future. *New Phytol.* **205**, 1406-1423 (2015).
- 505 15 Lindahl, B. D. & Tunlid, A. Ectomycorrhizal fungi—potential organic matter
506 decomposers, yet not saprotrophs. *New Phytol.* **205**, 1443-1447 (2015).
- 507 16 Liu, X. *et al.* Partitioning of soil phosphorus among arbuscular and ectomycorrhizal trees
508 in tropical and subtropical forests. *Ecol Lett* **21**, 713-723 (2018).
- 509 17 Zhu, K., McCormack, M. L., Lankau, R. A., Egan, J. F. & Wurzbarger, N. Association of
510 ectomycorrhizal trees with high carbon-to-nitrogen ratio soils across temperate forests is
511 driven by smaller nitrogen not larger carbon stocks. *Journal of Ecology* **106**, 524-535
512 (2018).
- 513 18 Binkley, D., Sollins, P., Bell, R., Sachs, D. & Myrold, D. Biogeochemistry of adjacent
514 conifer and alder-conifer stands. *Ecology* **73**, 2022-2033 (1992).
- 515 19 Leake, J. *et al.* Networks of power and influence: the role of mycorrhizal mycelium in
516 controlling plant communities and agroecosystem functioning. *Canadian Journal of*
517 *Botany* **82**, 1016-1045 (2004).
- 518 20 Hedin, L. O., Brookshire, E. N. J., Menge, D. N. L. & Barron, A. R. in *Annual Review of*
519 *Ecology Evolution and Systematics* Vol. 40 *Annual Review of Ecology Evolution and*
520 *Systematics* 613-635 (Annual Reviews, 2009).
- 521 21 Read, D. J. Mycorrhizas in Ecosystems. *Experientia* **47**, 376-391, doi:Doi
522 10.1007/Bf01972080 (1991).

523 22 Houlton, B. Z., Wang, Y.-P., Vitousek, P. M. & Field, C. B. A unifying framework for
524 dinitrogen fixation in the terrestrial biosphere. *Nature* **454**, 327 (2008).

525 23 Bueno, C. G. *et al.* Plant mycorrhizal status, but not type, shifts with latitude and
526 elevation in Europe. *Global Ecology and Biogeography* **26**, 690-699 (2017).

527 24 Soudzilovskaia, N. A., Vaessen, S., van't Zelfde, M. & Raes, N. in *Biogeography of*
528 *Mycorrhizal Symbiosis* 223-235 (Springer, 2017).

529 25 Brundrett, M. C. & Tedersoo, L. Evolutionary history of mycorrhizal symbioses and
530 global host plant diversity. *New Phytol.* (2018).

531 26 Peay, K. G. The mutualistic niche: mycorrhizal symbiosis and community dynamics.
532 *Annual Review of Ecology, Evolution, and Systematics* **47**, 143-164 (2016).

533 27 Pellegrini, A. F., Staver, A. C., Hedin, L. O., Charles-Dominique, T. & Tourgee, A.
534 Aridity, not fire, favors nitrogen-fixing plants across tropical savanna and forest biomes.
535 *Ecology* **97**, 2177-2183 (2016).

536 28 Liang, J. *et al.* Positive biodiversity-productivity relationship predominant in global
537 forests. *Science* **354**, aaf8957 (2016).

538 29 Brundrett, M. C. Mycorrhizal associations and other means of nutrition of vascular
539 plants: understanding the global diversity of host plants by resolving conflicting
540 information and developing reliable means of diagnosis. *Plant and Soil* **320**, 37-77,
541 doi:10.1007/s11104-008-9877-9 (2009).

542 30 Werner, G. D., Cornwell, W. K., Cornelissen, J. H. & Kiers, E. T. Evolutionary signals of
543 symbiotic persistence in the legume–rhizobia mutualism. *Proceedings of the National*
544 *Academy of Sciences* **112**, 10262-10269 (2015).

545 31 Afkhami, M. E. *et al.* Symbioses with nitrogen-fixing bacteria: nodulation and
546 phylogenetic data across legume genera. *Ecology* **99**, 502-502 (2018).

547 32 Tedersoo, L. *et al.* Global database of plants with root-symbiotic nitrogen fixation: Nod
548 DB. *Journal of Vegetation Science* (2018).

549 33 Wang, B. & Qiu, Y.-L. Phylogenetic distribution and evolution of mycorrhizas in land
550 plants. *Mycorrhiza* **16**, 299-363 (2006).

551 34 McGuire, K. *et al.* Dual mycorrhizal colonization of forest-dominating tropical trees and
552 the mycorrhizal status of non-dominant tree and liana species. *Mycorrhiza* **18**, 217-222
553 (2008).

554 35 Palosuo, T., Liski, J., Trofymow, J. & Titus, B. Litter decomposition affected by climate
555 and litter quality—testing the Yasso model with litterbag data from the Canadian intersite
556 decomposition experiment. *Ecological Modelling* **189**, 183-198 (2005).

557 36 Tuomi, M. *et al.* Leaf litter decomposition—estimates of global variability based on
558 Yasso07 model. *Ecological Modelling* **220**, 3362-3371 (2009).

559 37 Bradford, M. A. *et al.* Climate fails to predict wood decomposition at regional scales.
560 *Nature Climate Change* **4**, 625 (2014).

561 38 Ma, Z. *et al.* Evolutionary history resolves global organization of root functional traits.
562 *Nature* (2018).

563 39 Staver, A. C., Archibald, S. & Levin, S. Tree cover in sub-Saharan Africa: rainfall and
564 fire constrain forest and savanna as alternative stable states. *Ecology* **92**, 1063-1072
565 (2011).

566 40 Scheffer, M., Carpenter, S., Foley, J. A., Folke, C. & Walker, B. Catastrophic shifts in
567 ecosystems. *Nature* **413**, 591 (2001).

568 41 Parmesan, C. & Yohe, G. A globally coherent fingerprint of climate change impacts
569 across natural systems. *Nature* **421**, 37 (2003).

570 42 Reich, P. B. & Oleksyn, J. Climate warming will reduce growth and survival of Scots
571 pine except in the far north. *Ecol Lett* **11**, 588-597, doi:10.1111/j.1461-
572 0248.2008.01172.x (2008).

573 43 Fernandez, C. W. & Kennedy, P. G. Revisiting the 'Gadgil effect': do interguild fungal
574 interactions control carbon cycling in forest soils? *New Phytol.* **209**, 1382-1394,
575 doi:10.1111/nph.13648 (2016).

576 44 Reich, P. B. *et al.* Geographic range predicts photosynthetic and growth response to
577 warming in co-occurring tree species. *Nature Climate Change* **5**, 148 (2015).

578 45 Hanewinkel, M. & Peyron, J.-L. Tackling climate change—the contribution of scientific
579 knowledge in forestry. *Ann Forest Sci* **71**, 113-115 (2014).

580 46 Vitousek, P. M. Litterfall, nutrient cycling, and nutrient limitation in tropical forests.
581 *Ecology* **65**, 285-298 (1984).

582 47 McGroddy, M. E., Daufresne, T. & Hedin, L. O. Scaling of C: N: P stoichiometry in
583 forests worldwide: Implications of terrestrial redfield-type ratios. *Ecology* **85**, 2390-2401
584 (2004).

585 48 Reich, P. B. & Oleksyn, J. Global patterns of plant leaf N and P in relation to temperature
586 and latitude. *Proceedings of the National Academy of Sciences of the United States of*
587 *America* **101**, 11001-11006 (2004).

588 49 Vitousek, P. M. & Sanford Jr, R. L. Nutrient cycling in moist tropical forest. *Annu Rev*
589 *Ecol Syst* **17**, 137-167 (1986).

590 50 Grunwald, S., Thompson, J. & Boettinger, J. Digital soil mapping and modeling at
591 continental scales: Finding solutions for global issues. *Soil Science Society of America*
592 *Journal* **75**, 1201-1213 (2011).

593 51 Corrales, A., Mangan, S. A., Turner, B. L. & Dalling, J. W. An ectomycorrhizal nitrogen
594 economy facilitates monodominance in a neotropical forest. *Ecol Lett* **19**, 383-392,
595 doi:10.1111/ele.12570 (2016).

596 52 Menge, D. N., Lichstein, J. W. & Ángeles-Pérez, G. Nitrogen fixation strategies can
597 explain the latitudinal shift in nitrogen-fixing tree abundance. *Ecology* **95**, 2236-2245
598 (2014).

599 53 Ter Steege, H. *et al.* Continental-scale patterns of canopy tree composition and function
600 across Amazonia. *Nature* **443**, 444 (2006).

601 54 Menge, D. N. *et al.* Why are nitrogen-fixing trees rare at higher compared to lower
602 latitudes? *Ecology* **98**, 3127-3140 (2017).

603 55 Liao, W., Menge, D. N., Lichstein, J. W. & Ángeles-Pérez, G. Global climate change will
604 increase the abundance of symbiotic nitrogen-fixing trees in much of North America.
605 *Global Change Biol* (2017).

606 56 Gei, M. *et al.* Legume abundance along successional and rainfall gradients in Neotropical
607 forests. *Nature ecology & evolution*, 1 (2018).

608